ENHANCING ROBOTIC MANIPULATION THROUGH FULLY INTEGRATED QUANTUM ANNEALING: THE FIQA-RM SYSTEM

Anonymous authors
Paper under double-blind review

ABSTRACT

This work explores the application of quantum annealing to enhance robotic manipulation systems. Specifically, we aim to theoretically illustrate how QA can be employed to optimize robotic manipulation tasks. By formulating problems using either Quadratic Unconstrained Binary Optimization or Ising models, we introduce the Fully Integrated Quantum Annealing for Robotic Manipulation (FIQA-RM) system. This system utilizes D-Wave's quantum annealer to effectively address complex optimization challenges in robotic manipulation. Our approach demonstrates the feasibility of optimizing robotic systems using quantum annealing techniques.

1 INTRODUCTION

Robotic manipulation represents a cornerstone of contemporary robotics research, with substantial implications for industrial automation, healthcare, and service robotics Billard & Kragic (2019); Mason (2018); Hägele et al. (2016); Holland et al. (2021); Hussain (2024). Optimization plays an important role in robotic manipulation, as it involves finding the most efficient ways to execute tasks under various constraints and uncertainties. Many problems in robotics are inherently NP-hard, meaning they are computationally intensive and lack efficient solutions that can be found in polynomial time. Examples of such problems include path planning, task scheduling, and grasp planning. The NP-hard nature of these problems necessitates the use of advanced optimization algorithms and heuristics to find approximate solutions within a reasonable timeframe. However, accurately simulating the manipulation of soft and deformable objects remains an open problem Almaghout & Klimchik (2024).

Quantum Annealing (QA) Salloum et al. (2024b); Morita & Nishimori (2008); Rajak et al. (2023); Yarkoni et al. (2022), a quantum computing Karim Eddin et al. (2024); Salloum et al. (2024a); Salloum et al. paradigm that utilizes the principles of quantum mechanics (as shown in Figure 1), offers promising solutions to the complex optimization problems inherent in robotic manipulation. Quantum annealers, like those developed by D-Wave Systems, can explore vast solution spaces efficiently, providing optimal configurations for given problems. This capability is particularly advantageous for robotic manipulation, where rapid and accurate optimization can significantly enhance performance.

In this context, the integration of QA into robotic manipulation systems addresses several persistent challenges, including motion planning, manipulator dynamics, and vision processing. QA can optimize these processes, providing solutions within feasible time frames, leading to substantial economic benefits, increased productivity, and reduced operational costs.

To the best of the authors' knowledge, the application of QA in the field of robotics is notably rare, and there may be no existing work integrating QA into manipulator robotic systems. Moreover, the recent demonstration by D-Wave Inc. of computational supremacy in quantum simulation King et al. (2024); D-Wave Systems; The Quantum Insider; Quantum Zeitgeist marks a pivotal milestone in the realm of quantum computing. Their success in simulating the non-equilibrium dynamics of a magnetic spin system, particularly through a quantum phase transition, underscores the remarkable power and efficiency of QA in confronting intricate optimization tasks that elude classical computers Preskill (2018); Vasseur & Moore (2016); Bauer et al. (2020); Georgescu et al. (2014)

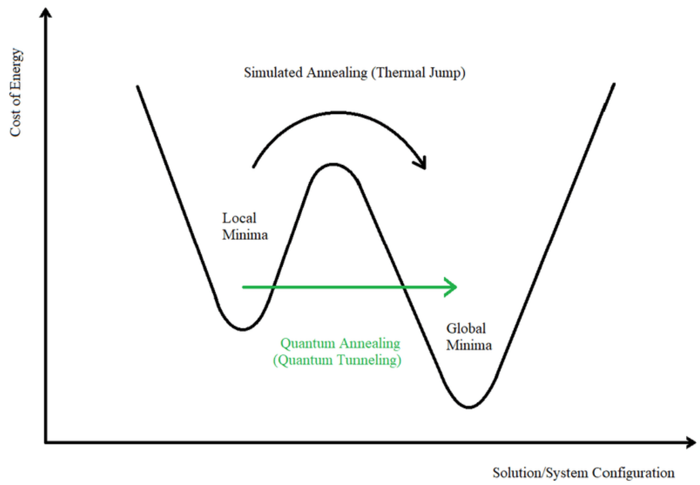

Figure 1: This graph shows the the advantage of quantum annealing over simulated annealing. Adapted form Sharma & Maharjan (2018)

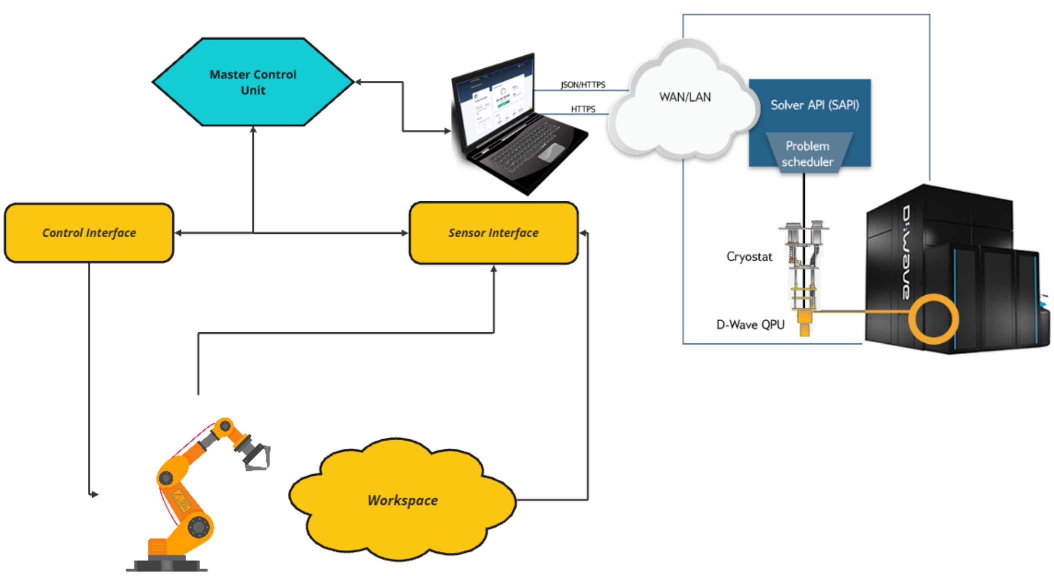

Figure 2: The FIQA-RM System Architecture

Therefore, our main contribution is to explore the application of QA in the field of robotics. Specifically, we aim to theoretically illustrate how robotic manipulation systems can be optimized using QA. By achieving either QUBO or Ising formulation, we demonstrate the FIQA-RM System (see Figure 2), which efficiently solves robotic manipulation problems using D-Wave's quantum annealer. This approach demonstrates how robotic manipulation systems can be effectively optimized for QA applications.

The paper structure is as follows: Section 2 presents the QA models for manipulator applications, covering three case studies: manipulation of deformable linear objects, manipulator dynamics, and stereo matching. In Section 3, the conclusion and future outlook are provided.

2 QA MODELS FOR MANIPULATOR APPLICATIONS

QA utilizes the Ising model Kadowaki & Nishimori (1998); Morita & Nishimori (2008); Santoro et al. (2002); McMahon (2007), which can be represented mathematically as follows:

$$\hat{H}_{\text{Ising}} = -\sum_i h_i \hat{\sigma}_i^z - \sum_{i<j} J_{ij} \hat{\sigma}_i^z \hat{\sigma}_j^z \tag{1}$$

where $\hat{\sigma}_i^z$ are Pauli Z matrices representing the spin variables, h_i are local fields, and J_{ij} are coupling constants between spins. the Hamiltonian for the transverse-field Ising model used in QA:

$$\hat{H}(t) = -A(t) \sum_i \hat{\sigma}_i^x + B(t) \hat{H}_{\text{Ising}} \tag{2}$$

where $A(t)$ and $B(t)$ are annealing schedules, and $\hat{\sigma}_i^x$ are Pauli X matrices. The time-dependent Hamiltonian $\hat{H}(t)$ interpolates between the initial Hamiltonian and the problem Hamiltonian.

We can further refine this to include the complexities of robotic manipulation by incorporating additional terms to the Hamiltonian that model various interaction potentials and constraints. For example, a more comprehensive Hamiltonian might take the form:

$$\hat{H}(t) = -A(t) \sum_i \hat{\sigma}_i^x + B(t) \left(-\sum_i h_i \hat{\sigma}_i^z - \sum_{i<j} J_{ij} \hat{\sigma}_i^z \hat{\sigma}_j^z + \sum_{i,j,k} K_{ijk} \hat{\sigma}_i^z \hat{\sigma}_j^z \hat{\sigma}_k^z + \sum_i g_i \hat{\sigma}_i^x \hat{\sigma}_i^z \right) \tag{3}$$

where K_{ijk} are higher-order interaction terms and g_i are additional local field terms that could represent external constraints or interactions.

In the context of QUBO, the Ising model can be reformulated as:

$$E(\mathbf{s}) = \mathbf{s}^T \mathbf{Q} \mathbf{s} = \sum_i Q_{ii} s_i + \sum_{i<j} Q_{ij} s_i s_j \tag{4}$$

where $\mathbf{s}$ is a vector of binary variables, and $\mathbf{Q}$ is a matrix encoding the problem's constraints and interactions. The goal is to find the binary vector $\mathbf{s}$ that minimizes the energy function $E(\mathbf{s})$.

Following in this paper, we address three key robotics applications:

2.1 MANIPULATION OF DEFORMABLE LINEAR OBJECTS (DLOS)

The robot controller is formulated as an optimization problem, where the main objective is to minimize the error between the current shape and the desired shape, while ensuring the diminishing rigidity property of the DLO as a constraint. In the work Almaghout et al. (2024), the intermediary shapes generation (ISG) algorithm takes the initial and desired shapes (each represented as a set of points), and generates intermediary shapes which can be considered as local desired shapes. Once these intermediary shapes are generated, the robots guide the DLO from the current shape to the desired shape through these intermediary ones, but in our work, we will consider form the work Almaghout et al. (2024) the robots' motion which is planned as an optimization control problem (OCP), where the desired displacement of the robot end-effectors is computed to minimize the error between the current DLO shape and the next intermediary shape, in an iterative manner towards the desired shape.

Let us consider two robotic arms rigidly grasping a DLO at its two ends. The robots cooperatively manipulate the DLO on a 2D plane to move it from an initial to a desired shape. The problem is to design the robots' controller to guide the DLO towards its desired shape as shown in Figure 3.

This task will be formulated as a QUBO problem by modeling the interactions between the robot and the deformable object taking into account the DLO physical constraints. The objective is to

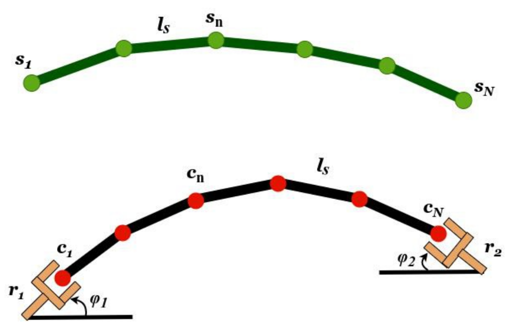

Figure 3: Illustrious of the manipulation of DLO problem. Adapted from Almaghout et al. (2024).

convert the optimization control problem (OCP) for DLO manipulation into a QUBO problem. The original OCP, which consider that the cable is represented at a set of N points connected by rigid links, is given by:

$$\min_{\mathbf{r}} \sum_{n=1}^{N} \|\mathbf{c}_n^{\kappa} - \mathbf{c}_n\| \tag{5}$$

subject to:

$$\dot{\mathbf{c}} = \mathbf{J}\dot{\mathbf{r}} \tag{6}$$

$$|\dot{\mathbf{r}}| \leq \nu \tag{7}$$

where κ is the next local desired shape, $\mathbf{c} = [\mathbf{c}_1, \mathbf{c}_2, \cdots, \mathbf{c}_N]^T$ and $\mathbf{s} = [\mathbf{s}_1, \mathbf{s}_2, \cdots, \mathbf{s}_N]^T \in \mathbb{R}^{2N}$ are the vectors of DLO point coordinates and desired shape point coordinates, respectively. For each $n = 1, 2, \ldots, N$:

$$\mathbf{c}_n = \begin{bmatrix} c_{nx} \\ c_{ny} \end{bmatrix} \quad \text{and} \quad \mathbf{s}_n = \begin{bmatrix} s_{nx} \\ s_{ny} \end{bmatrix}$$

The robots' end-effectors configurations are defined by the vector $\mathbf{r} = [\mathbf{r}_1, \mathbf{r}_2]^T \in \mathbb{R}^6$, where for $m = 1, 2$:

$$\mathbf{r}_m = \begin{bmatrix} r_{mx} \\ r_{my} \\ \phi_m \end{bmatrix}$$

To transform this OCP (eq 5, 6, and 7) into a QUBO problem, we utilize the Laplace transform which is a powerful mathematical tool used to convert differential equations into algebraic equations, simplifying their analysis and solution.

Applying the Laplace transform to both sides of equation 6, we use the property of the Laplace transform of derivatives:

$$\mathcal{L}\{\dot{c}(t)\} = sC(s) - c(0) \tag{8}$$

$$\mathcal{L}\{\dot{r}(t)\} = sR(s) - r(0) \tag{9}$$

Thus, the Laplace-transformed equation becomes:

$$sC(s) - c(0) = \mathbf{J} \cdot (sR(s) - r(0)) \tag{10}$$

Rearrange to solve for $C(s)$:

$$sC(s) - c(0) = \mathbf{J} \cdot sR(s) - \mathbf{J} \cdot r(0) \tag{11}$$

$$sC(s) = \mathbf{J} \cdot sR(s) + c(0) - \mathbf{J} \cdot r(0) \tag{12}$$

$$C(s) = \mathbf{J}R(s) + \frac{c(0) - \mathbf{J}r(0)}{s} \tag{13}$$

Here, $C(s)$ and $R(s)$ are the Laplace transforms of $c(t)$ and $r(t)$, respectively. $c(0)$ and $r(0)$ are the initial conditions of c and r, respectively.

Substituting $C(s)$ into equation 5:

$$\min_{R(s)} \sum_{n=1}^{N} \left\| \mathbf{J}R(s) + \frac{\mathbf{c}_{\mathbf{n}}^{\kappa}(0) - \mathbf{J}r(0) - c_n(0)}{s} \right\| \tag{14}$$

For the constraint $|\dot{r}| \leq \nu$, applying the Laplace transform yields:

$$|\mathcal{L}\{\dot{r}\}| = |sR(s) - r(0)| \leq \nu \tag{15}$$

To convert the continuous variable r into binary variables, let r be approximated by binary variables x_i:

$$s \approx \sum_{i=1}^{k} 2^{i-1} x_i \tag{16}$$

where x_i are binary variables (0 or 1), and w is the number of binary variables.

Substituting this approximation (eq 16) into equation 5:

$$\min_{R(s)} \sum_{n=1}^{N} \left(\mathbf{J} \left(\sum_{i=1}^{w} 2^{i-1} x_i \right) + \frac{\mathbf{c}_n^{\kappa}(0) - \mathbf{J}r(0) - c_n(0)}{s} \right)^2 \tag{17}$$

Let:

$$A_n = \mathbf{J} \tag{18}$$

$$B_n = \frac{\mathbf{c}_n^{\kappa}(0) - \mathbf{J}r(0) - c_n(0)}{s} \tag{19}$$

Then the objective function becomes:

$$\text{Objective} = \sum_{n=1}^{N} \left(A_n \sum_{i=1}^{w} 2^{i-1} x_i + B_n \right)^2 \tag{20}$$

Expanding the objective function:

$$\text{Objective} = \sum_{n=1}^{N} \left(A_n^2 \left(\sum_{i=1}^{w} 2^{i-1} x_i \right)^2 + 2A_n B_n \left(\sum_{i=1}^{w} 2^{i-1} x_i \right) + B_n^2 \right) \tag{21}$$

$$\text{Objective} = \sum_{n=1}^{N} \left(A_n^2 \sum_{i=1}^{k} \sum_{j=1}^{k} 2^{i-1} 2^{j-1} x_i x_j + 2A_n B_n \sum_{i=1}^{k} 2^{i-1} x_i + B_n^2 \right) \tag{22}$$

The constraint $|s\left(\sum_{i=1}^{w} 2^{i-1} x_i\right) - r(0)| \leq \nu$ is transformed into a penalty term. substituting eq 16 in eq 15, the constrained is given as:

$$\text{Penalty} = \lambda \left(\max \left(0, \left| s \left(\sum_{i=1}^{w} 2^{i-1} x_i \right) - r(0) \right| - \nu \right) \right)^2 \tag{23}$$

Approximate the penalty term as:

$$\text{Penalty} = \lambda \left(\left(s \sum_{i=1}^{w} 2^{i-1} x_i - r(0) \right)^2 - \nu^2 \right)^2 \tag{24}$$

Combining the objective function and penalty term, we get the final QUBO formulation:

$$\text{Q} = \sum_{n=1}^{N} \left(A_n^2 \sum_{i=1}^{w} \sum_{j=1}^{w} 2^{i-1} 2^{j-1} x_i x_j + 2A_n B_n \sum_{i=1}^{w} 2^{i-1} x_i + B_n^2 \right) + \lambda \left(\left(s \sum_{i=1}^{w} 2^{i-1} x_i - r(0) \right)^2 - \nu^2 \right)^2 \tag{25}$$

This QUBO formulation is suitable for implementation on the D-Wave quantum annealer, where it can find the minimum energy configuration.

2.2 Manipulator Dynamics

In this task, we aim to construct the motion equations for manipulators as QUBO problems. This involves formulating the dynamic constraints and control objectives of the robotic manipulators into a quadratic binary optimization problem. The QUBO formulation will address the optimization of motion trajectories and control inputs while adhering to dynamic constraints. The dynamics of a robotic manipulator, particularly for applications such as a robot inspector traversing a conductor, can be effectively modeled using the deflection equation of a stretched string, as described in Bahrami & Abed (2019):

$$Tu''(x,t) + f(x,t) = \rho u''(x,t) \tag{26}$$

In this equation, T signifies the tension force within the string, $f(x,t)$ denotes the linear load, ρ represents the density, and $u(x,t)$ indicates the deflection, with differentiation taken with respect to the spatial coordinate x and time t. The force is localized at the specific point $x = \xi$ using the delta function:

$$f(x,t) = F(t)\delta(x - \xi(t)) \tag{27}$$

The differential equation solution is derived using the Lagrange equations, which leads to a system of ordinary differential equations (ODEs):

$$q' = w \tag{28}$$

$$w' = M^{-1}(-Cq + Q(t)) \tag{29}$$

In the eq 28 and eq 29, q and w are the generalized coordinates and velocities, M is the kinetic energy matrix, C is the potential energy matrix, and $Q(t)$ represents the generalized forces determined from the principle of virtual work.

To solve these equations using a quantum annealer, we transform them into an Ising model Hamiltonian, beginning with a minimization problem Criado & Spannowsky (2022). The domains are discretized into finite subsets, and the loss function is defined as:

$$L[f] = \sum_i \sum_{x \in X_i} (E_i(x)[f])^2 \tag{30}$$

Here, X_i represents the subsets. The function f is parameterized as a linear combination of basis functions Φ_m, and the equations are rewritten as linear functions of the parameters w_{nm}:

$$E_i(x,w) = \sum_{nm} H_{in}(x)[\Phi_m] w_{nm} + B_i(x) \tag{31}$$

In this formulation, $B_i(x)$ represents the inhomogeneous terms. The loss function then becomes a quadratic function of the parameters:

$$L(w) = \sum_{n,m,p,q} w_{nm} \left(\sum_{i,x \in X_i} H_{in}(x)[\Phi_m] H_{ip}(x)[\Phi_q] \right) w_{pq} + \sum_{n,m} \left(2 \sum_{i,x \in X_i} H_{in}(x)[\Phi_m] B_i(x) \right) w_{nm} \tag{32}$$

The Ising model Hamiltonian $H(\hat{w})$ is derived by binary encoding of the weights using spin variables $\hat{w}(\alpha)_{nm} = \pm 1$:

$$\hat{w}nm = cnm + s_{nm} \sum_{\alpha=1}^{n_{\text{spin}}} \frac{\hat{w}(\alpha)_{nm}}{2^\alpha} \tag{33}$$

The solution is obtained by minimizing H on a QA device, and decoding the weights. The accuracy is improved through an iterative algorithm with a scaling factor S over multiple epochs.

This method involves several hyperparameters that need to be tuned based on the specific problem and the limitations of the QA device. These parameters, and their typical values, are discussed for efficiently solving differential equations.

This approach provides a novel way to solve complex differential equations using the computational power of QA. By transforming the equations into an Ising model Hamiltonian and solving them on QA devices, we can efficiently address problems that are challenging for classical computing methods.

2.3 STEREO MATCHING

Stereo matching is a fundamental problem in computer vision aimed at estimating depth by finding correspondences between pixels in two rectified stereo images Hamid et al. (2022); Hamzah & Ibrahim (2016). The optimization task involves assigning disparity values to pixels in the left image I_l to minimize an energy function that integrates data fidelity and smoothness constraints.

Given rectified stereo images I_l and I_r, each of dimensions $n \times m$, and a disparity set $D = \{d_{\text{min}}, d_{\text{min}} + 1, \ldots, d_{\text{max}}\}$, the objective is to minimize the energy function $F(\mathbf{w})$. Here, $\mathcal{Q}$ denotes a pair of index pairs $\{(i,j),(i',j')\}$, which defines the pairs used in the function δ. The function $F(\mathbf{w})$ is defined as:

$$F(\mathbf{w}) = \sum_{(i,j)\in P} \theta_{i,j}(w_{i,j}) + \lambda \sum_{\mathcal{Q}\in N} \delta(w_{i,j}, w_{i',j'}) \tag{34}$$

where:

- **Data Term $\theta_{i,j}(w_{i,j})$:**

  $$\theta_{i,j}(w_{i,j}) = \|I_l(i,j) - I_r(i - w_{i,j}, j)\| \tag{35}$$

  This term measures the cost of matching pixel intensities between the left and right images, ensuring that disparities minimize this mismatch.

- **Smoothness Term $\delta(w_{i,j}, w_{i',j'})$:**

  $$\delta(w_{i,j}, w_{i',j'}) = \begin{cases} 0, & \text{if } w_{i,j} = w_{i',j'} \\ 1, & \text{otherwise} \end{cases} \tag{36}$$

  This term enforces smoothness in disparity values, penalizing inconsistencies between neighboring pixels. The smoothness parameter λ adjusts the trade-off between data fidelity and smoothness.

The problem is converted to a QUBO format using binary variables $x_{i,j,d}$, where $x_{i,j,d}$ is 1 if pixel (i,j) is assigned disparity d, and 0 otherwise Heidari et al. (2024).

For our use case, we will have to modify the infeasibility penalty - it should be able to serve the images of an arbitrary size and color scale, never letting the infeasible solutions (for fixed i, j either zero or more than one $x_{i,j,d}$ are equal to 1) have less cost than feasible ones.

Let k be the number of color channels having integer values in $[0, 255]$ ($k = 3$ in RGB, $k = 1$ in grayscale) and $m \times n$ be the image size. P is the set of image pixel coordinates (i,j), N is the set of unordered adjacent pixel pairs $\{(i,j),(i',j')\}$, where $(i',j') \in \{(i \pm 1, j),(i, j \pm 1)\}$.

In feasible solutions, data term $\theta_{i,j}(w_{i,j})$ can go up to $255k$ for each pixel, as we consider the Manhattan distance between $[255 \ldots 255]^T$ and $[0 \ldots 0]^T$ vectors denoting pixel colors. Therefore, the sum of data terms over an $m \times n$ image shall not exceed $255kmn$.

The smoothness term considers all the elements of N. In $m \times n$ image, $|N| = 2mn - m - n$, then the smoothness cost over the image shall not exceed $\lambda(2mn - m - n)$, leading to the total penalty in feasible solutions not exceeding $255kmn + \lambda(2mn - m - n)$.

Then the QUBO model is:

$$
\begin{aligned}
H(\mathbf{x}) = (255kmn + \lambda(2mn - m - n)) \sum_{(i,j)\in P} (1 - \sum_{d\in D} x_{i,j,d})^2 \\
+ \sum_{(i,j)\in P} \sum_{d\in D} \theta_{i,j}(d) \cdot x_{i,j,d} \\
+ \lambda \sum_{\mathcal{Q}\in N} \sum_{d\in D} \sum_{d'\in D} \delta(d,d') \cdot x_{i,j,d} \cdot x_{i',j',d'}
\end{aligned} \tag{37}
$$

Components:

- **Infeasibility Penalty Term:**

$$(255kmn + \lambda(2mn - m - n)) \sum_{(i,j)\in P} \left(1 - \sum_{d\in D} x_{i,j,d}\right)^2 \tag{38}$$

  This term penalizes the assignment of multiple disparity values to a single pixel. The scaling factor $255kmn + \lambda(2mn - m - n)$ ensures that infeasible solutions are heavily penalized, maintaining the requirement that each pixel has exactly one disparity value.

- **Data Cost Term:**

$$\sum_{(i,j)\in P} \sum_{d\in D} \theta_{i,j}(d) \cdot x_{i,j,d} \tag{39}$$

  Incorporates the pixel matching cost, guiding the optimization to minimize the intensity differences between corresponding pixels in the stereo images.

- **Smoothness Cost Term:**

$$\lambda \sum_{\mathcal{Q}\in N} \sum_{d\in D} \sum_{d'\in D} \delta(d,d') \cdot x_{i,j,d} \cdot x_{i',j',d'} \tag{40}$$

  Penalizes disparity variations between neighboring pixels, with the penalty size determined by the smoothness parameter λ. A higher λ promotes larger regions with consistent disparity values.

Therefore, the D-Wave quantum annealer, by utilizing the QUBO formulation, can effectively find the optimal solution to the problem by identifying the minimum energy configuration.

3 Conclusion & Future Work

In this work, we have successfully formulated complex robotic manipulation problems as Quadratic Unconstrained Binary Optimization (QUBO) models. The formulations cover key areas such as manipulator dynamics, stereo matching, and the handling of deformable linear objects (DLOs). These QUBO models are designed to leverage the capabilities of QA to address optimization challenges in robotic systems. Future work will focus on extending this research through extensive experimental validation. We aim to conduct comprehensive experiments to evaluate the effectiveness of our QUBO formulations in practical scenarios. Additionally, we will compare the performance of our quantum-optimized models with state-of-the-art classical methods to assess their relative advantages and limitations. This comparison will provide valuable insights into the practical benefits and potential improvements of QA for robotic manipulation applications.

Acknowledgments

This research has been financially supported by The Analytical Center for the Government of the Russian Federation (Agreement No. 70-2021-00143 dd. 01.11.2021, IGK 000000D730321P5Q0002)).

REFERENCES

Karam Almaghout and Alexandr Klimchik. Manipulation planning for cable shape control. *Robotics*, 13(1):18, 2024.

Karam Almaghout, Andrea Cherubini, and Alexandr Klimchik. Robotic co-manipulation of deformable linear objects for large deformation tasks. *Robotics and Autonomous Systems*, pp. 104652, 2024.

M. R. Bahrami and S. A. Abed. Mechanics of robot inspector on electrical transmission lines conductors: performance analysis of dynamic vibration absorber. *Vibroengineering Procedia*, 25: 60–64, 2019.

Bela Bauer, Sergey Bravyi, Mario Motta, and Garnet Kin-Lic Chan. Quantum algorithms for quantum chemistry and quantum materials science. *Chemical Reviews*, 120(22):12685–12717, 2020.

Aude Billard and Danica Kragic. Trends and challenges in robot manipulation. *Science*, 364(6446): eaat8414, 2019.

J. C. Criado and M. Spannowsky. Qade: solving differential equations on quantum annealers. *Quantum Science and Technology*, 8(1):015021, 2022.

D-Wave Systems. Computational supremacy in quantum simulation. `https://www.dwavesys.com/resources/publication/computational-supremacy-in-quantum-simulation/`. Accessed: May 26, 2024.

Iulia M. Georgescu, Sahel Ashhab, and Franco Nori. Quantum simulation. *Reviews of Modern Physics*, 86(1):153, 2014.

Martin Hägele, Klas Nilsson, J Norberto Pires, and Rainer Bischoff. Industrial robotics. *Springer handbook of robotics*, pp. 1385–1422, 2016.

Mohd Saad Hamid, NurulFajar Abd Manap, Rostam Affendi Hamzah, and Ahmad Fauzan Kadmin. Stereo matching algorithm based on deep learning: A survey. *Journal of King Saud University-Computer and Information Sciences*, 34(5):1663–1673, 2022.

Rostam Affendi Hamzah and Haidi Ibrahim. Literature survey on stereo vision disparity map algorithms. *Journal of Sensors*, 2016(1):8742920, 2016.

Shahrokh Heidari, Michael J Dinneen, and Patrice Delmas. Quantum annealing for computer vision minimization problems. *Future Generation Computer Systems*, 2024.

Jane Holland, Liz Kingston, Conor McCarthy, Eddie Armstrong, Peter O'Dwyer, Fionn Merz, and Mark McConnell. Service robots in the healthcare sector. *Robotics*, 10(1):47, 2021.

Shafiq Hussain. Potential of robot manipulation across diverse fields. *Integrated Journal of Science and Technology*, 1(5), 2024.

Tadashi Kadowaki and Hidetoshi Nishimori. Quantum annealing in the transverse ising model. *Physical Review E*, 58(5):5355, 1998.

Suleiman Karim Eddin, Hadi Salloum, Mohamad Nour Shahin, Badee Salloum, Manuel Mazzara, and Mohammad Reza Bahrami. Quantum microservices: transforming software architecture with quantum computing. In *International Conference on Advanced Information Networking and Applications*, pp. 227–237. Springer, 2024.

A. D. King, A. Nocera, M. M. Rams, J. Dziarmaga, R. Wiersema, W. Bernoudy, J. Raymond, N. Kaushal, N. Heinsdorf, and et al. R. Harris. Computational supremacy in quantum simulation. *arXiv preprint arXiv:2403.00910*, 2024.

Matthew T Mason. Toward robotic manipulation. *Annual Review of Control, Robotics, and Autonomous Systems*, 1(1):1–28, 2018.

David McMahon. *Quantum computing explained*. John Wiley & Sons, 2007.

Satoshi Morita and Hidetoshi Nishimori. Mathematical foundation of quantum annealing. *Journal of Mathematical Physics*, 49(12), 2008.

John Preskill. Quantum computing in the nisq era and beyond. *Quantum*, 2:79, 2018.

Quantum Zeitgeist. D-wave claims quantum advantage in new research. https://quantumzeitgeist.com/d-wave-claims-quantum-advantage-in-new-research/. Accessed: 2024.

Atanu Rajak, Sei Suzuki, Amit Dutta, and Bikas K Chakrabarti. Quantum annealing: An overview. *Philosophical Transactions of the Royal Society A*, 381(2241):20210417, 2023.

Hadi Salloum, Ruslan Lukin, and Manuel Mazzara. Quantum computing in drug discovery: A review of quantum annealing and gate-based approaches. In *International Conference on Computational Optimization*.

Hadi Salloum, Murhaf Alawir, Mohammad Anas Alatasi, Saleem Asekrea, Manuel Mazzara, and Mohammad Reza Bahrami. Quantum advancements in securing networking infrastructures. In *International Conference on Advanced Information Networking and Applications*, pp. 354–363. Springer, 2024a.

Hadi Salloum, Hamza Shafee Aldaghstany, Osama Orabi, Ahmad Haidar, Mohammad Reza Bahrami, and Manuel Mazzara. Integration of machine learning with quantum annealing. In *International Conference on Advanced Information Networking and Applications*, pp. 338–348. Springer, 2024b.

Giuseppe E Santoro, Roman Martoňák, Erio Tosatti, and Roberto Car. Theory of quantum annealing of an ising spin glass. *Science*, 295(5564):2427–2430, 2002.

A Sharma and Pradip Maharjan. Quantum annealing as an optimized simulated annealing: a case study, 2018.

The Quantum Insider. D-wave-led research team reports on quantum advantage in quantum simulation task. https://thequantuminsider.com/2024/03/07/d-wave-led-research-team-reports-on-quantum-advantage-in-quantum-simulation-task/. Accessed: March 7, 2024.

Romain Vasseur and Joel E. Moore. Nonequilibrium quantum dynamics and transport: from integrability to many-body localization. *Journal of Statistical Mechanics: Theory and Experiment*, 2016(6):064010, 2016.

Sheir Yarkoni, Elena Raponi, Thomas Bäck, and Sebastian Schmitt. Quantum annealing for industry applications: Introduction and review. *Reports on Progress in Physics*, 85(10):104001, 2022.